http://doi.org/10.24867/JPE-2022-01-005

Journal of Production Engineering

Vol.25 No.1

JPE (2022) Vol.25 (1) Original Scientific Paper

Bodzás, S.

FEM ANALYSIS OF THE TOOTH OF PINIONS IN CASE OF BEVEL GEARS HAVING THE MODIFICATION OF THE SHAFT ANGLES BY THE CHANGING OF LOAD FORCES

Received: 23 March 2022 / Accepted: 17 May 2022

Abstract: *Five types of bevel gears having different shaft angles were designed. In this publication the analysis of the tooth of pinions will be focused. Different load forces will be loaded on the top of the tooth on the surfaces of the face cones. The normal stresses and normal deformations of one tooth will be analysed into two perpendicular directions on both tooth sides. The aim is the foundation of the correlation between the mechanical parameters and the shaft angles by the different load forces.*
Key words: *Tooth, bevel gear, load force, FEM, normal, pitch angle.*

FEM analiza zuba zupčanika u slučaju konusnih zupčanika koji imaju modifikaciju uglova vratila promenom sila opterećenja. *Projektovano je pet tipova konusnih zupčanika sa različitim uglovima osovine. U ovoj publikaciji biće fokusirana analiza zuba zupčanika. Različite sile opterećenja će biti opterećene vrhom zuba na površinama čeonih konusa. Normalni naponi i normalne deformacije jednog zuba će se analizirati u dva okomita pravca sa obe strane zuba. Cilj je utvrđivanje korelacije između mehaničkih parametara i uglova osovine različitim silama opterećenja.*
Key words: *Zub, konusni zupčanik, sila opterećenja, FEM, normalan, ugao nagiba.*

1. INTRODUCTION

The bevel gear pairs are used in many areas in the engineering constructions. The aims of these gear are the high power transmission and the shaft between the shafts [1, 5-12, 14-21]. This angle can be different which is depended on the machine construction and the assembly position (Figure 1).

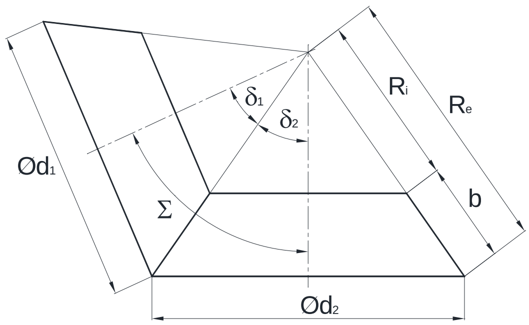

a) theoretical figure [6]

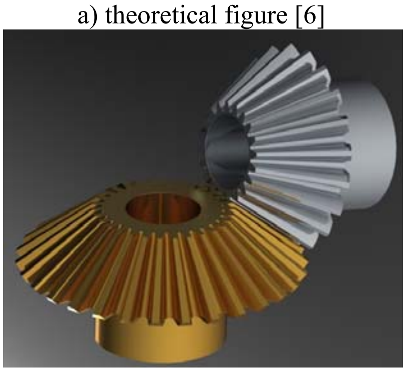

b) CAD model of our designed gear pair (Σ=80°)

Fig. 1. The significance of the shaft angle in case of design of bevel gears

The formula for the calculation of the shaft angle if Σ<90° is [6]:

$$cot\delta_2 = \frac{z_1}{z_2 \cdot sin\Sigma} \cdot cot\Sigma \quad (1)$$

Five types of gear pairs have been designed [2, 3]. The difference is only the shaft angle between the connecting elements. This parameter were modified between 70° - 90° by 5° degree's discreet steps. The main parameters of them are contained in [2, 3] publications.

The geometric designing was made by GearTeq software [2, 3, 4]. This software is fairly complex because of the many designing possibilities and options. Knowing of the suggested designing principles [1, 5-12, 14-21] many types of gears (spur gear, helical gear, bevel gear, worm gear, etc.) can be designed. After the setting of the input designing parameters [5, 6, 12, 15, 21] this software can calculate the other necessary parameters which are needed for the designing and the manufacturing considering the theorem of double wrapping [8, 9, 10, 12]. Knowing of the geometry of the pinion or the driven gear this software can determine the geometric surface of the missing component with the necessary parameters [4].

After the designing the parameters can be saved into the Solidworks where the designed gear pair can be visualized. If it is necessary, the outside geometric parameters can be modified. The motion simulation is one of the most important area of the gear designing where the exact tooth connection between the components can be checked by kinematical motions [1, 8, 9, 18]. After the checking the TCA can be followed

[1, 7, 8, 9, 12, 14, 16-20] where the mechanical parameters can be analysed by different loads.

In this research we analyse the tooth of the pinion of these gear pairs in the function of the load forces. We analyse the normal deformations and normal stresses in many directions and search correlations between the mechanical parameters and the shaft angles by different load forces.

2. FEM ANALYSIS OF THE TOOTH OF THE PINION

The first step of the analysis is the determination of the necessary coordination systems where the mechanical parameters (normal stresses and deformations) can be analysed (Figure 2) [13].

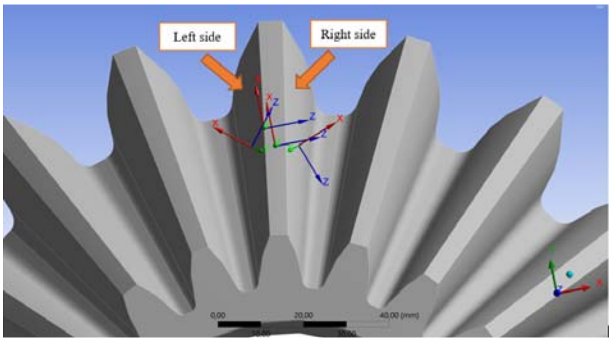

Fig. 2. The arrangement of the coordinate system

Four coordinate systems are needed. Two coordinate systems were defined on the left and right tooth sides. The *'x'* directions of them are the normal vectors of the surface. The *'y'* directions of them are shown into the axial direction of the centre hole. One coordinate system is needed for the definition of the centre of the sphere because sphere meshing was used. This system is situated on the middle of the tooth. Finally, one coordinate system is needed for the definition of the load forces. This system is situated on the intersection line of the side surface and the face cone (Figure 2).

The selected material type was structural steel [2, 3]. Sphere meshing [13] were used having 1 mm element size and 65 mm sphere radius on the analysed area (Figure 3). Automatic meshing were used on the outside areas.

The load forces [13] were defined on the *'x'* and *'z'* directions accordingly Figure 4 for the analysis. The centre hole of the pinion was fixed. The load force was changed form 500 N to 2500 N having 500 N discreet steps.

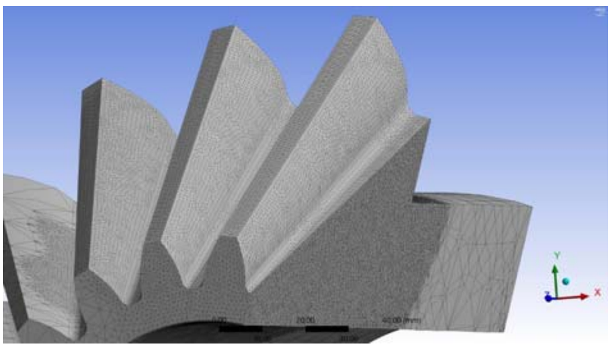
Fig. 3. The FEM mesh of the analysed tooth

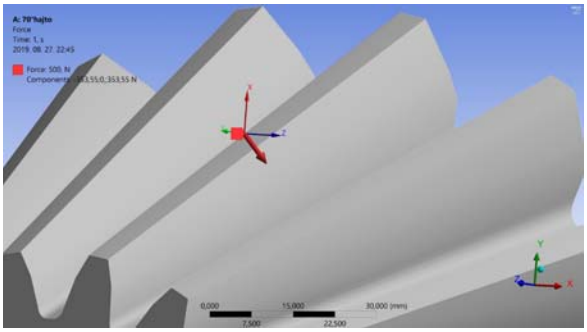
Fig. 4. Definition of the load force

2.1 The analysis of the normal stresses

The normal stresses were analysed into *'x'* and *'y'* directions for both tooth sides accordingly Figure 2. Naturally this analyses were done for all of bevel gear pairs (Σ=70°-90°).

2.1.1. 'x' direction, left side

The distributions of normal stress into *'x'* direction can be seen on Figure 5 on the left side. This direction is the normal direction of this tooth side. Based on Table 1 and Figure 6 the highest normal stress values were appeared in case of Σ=90° arrangement in absolute value. The lowest normal stress values were appeared in case of Σ=75° arrangement in absolute value. The shapes of the diagrams are approximately linear.

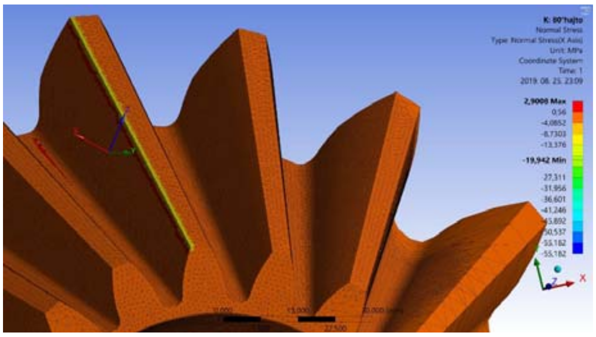
a) F=500 N

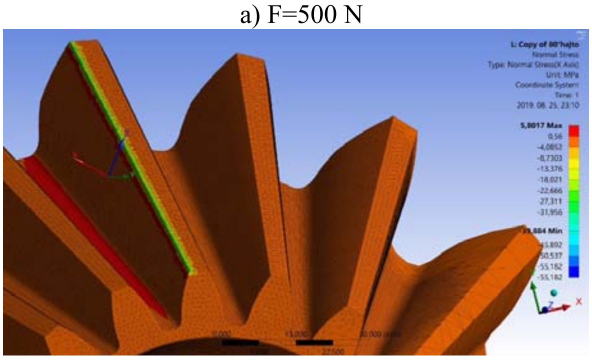
b) F=1000 N

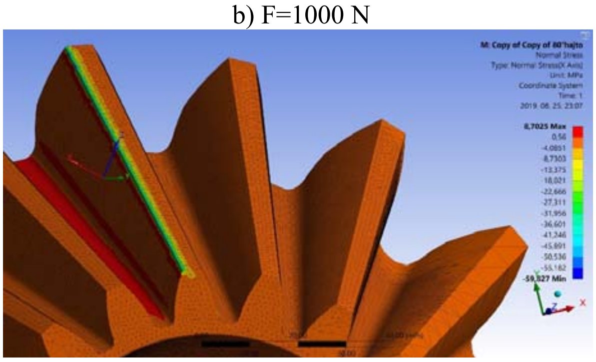
c) F=1500 N

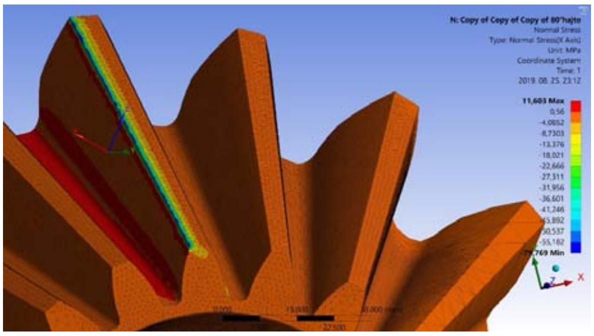

d) F=2000 N

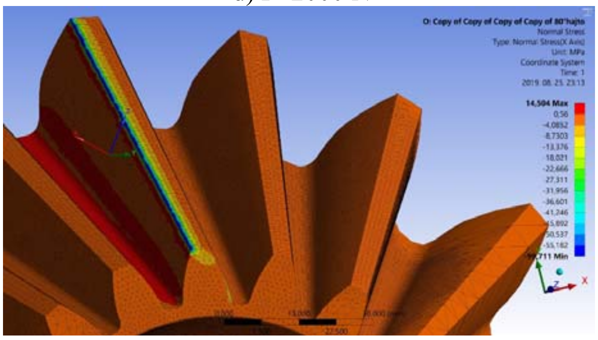

e) F=2500 N

Fig. 5. The distributions of the normal stress in the function of the load forces (Σ=80°, *'x'* direction, left side)

Load force (N)	Shaft angle (°)				
	70°	**75°**	**80°**	**85°**	**90°**
500	-0.468	-0.457	-0.474	-0.465	-0.474
1000	-0.936	-0.914	-0.948	-0.93	-0.951
1500	-1.405	-1.371	-1.422	-1.395	-1.427
2000	-1.873	-1.829	-1.896	-1.86	-1.902
2500	-2.342	-2.286	-2.37	-2.326	-2.378

Table 1. The distributions of the *'x'* directional normal stress (MPa) on the left side

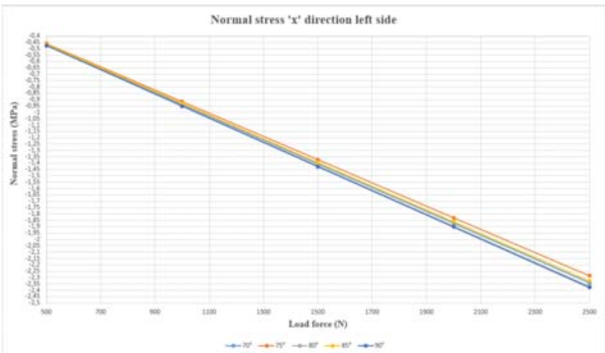

Fig. 6. The function of the normal stress and the load force for different shaft angles (*'x'* direction, left side)

Load force (N)	Deviation between the results (%)
500	4
1000	4
1500	4
2000	4
2500	4

Table 2. The deviations between the highest and the lowest results

The results between the Σ=90° and Σ=75° arrangements can be seen on Table 2 in percentage. The deviations between the highest and lowest results are 4% in both cases.

2.1.2. 'y' direction, left side

The distributions of the normal stress into *'y'* direction can be seen on Figure 7 on the left side. This direction is the axial direction.

Based on Table 3 and Figure 8 the highest normal stress values were appeared in case of Σ=90° arrangement. The lowest normal stress values were appeared in case of Σ=70° arrangement. The shape of the diagrams is approximately linear.

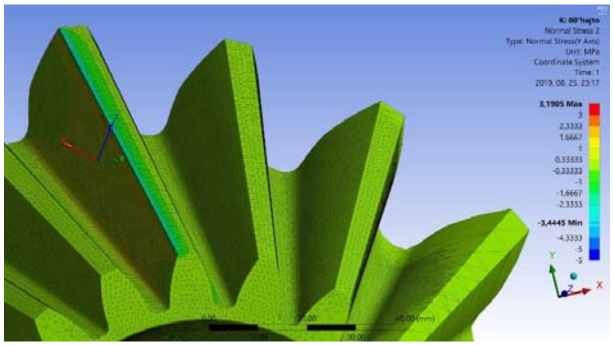

a) F=500N

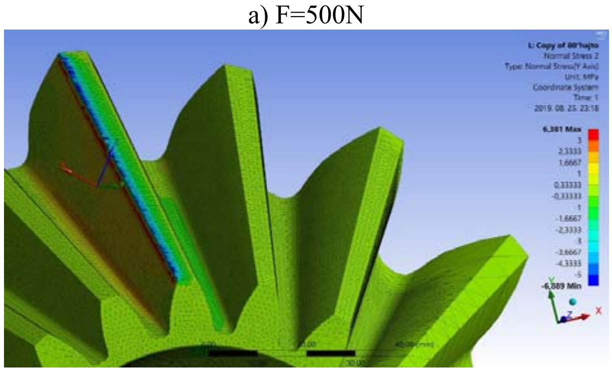

b) F=1000N

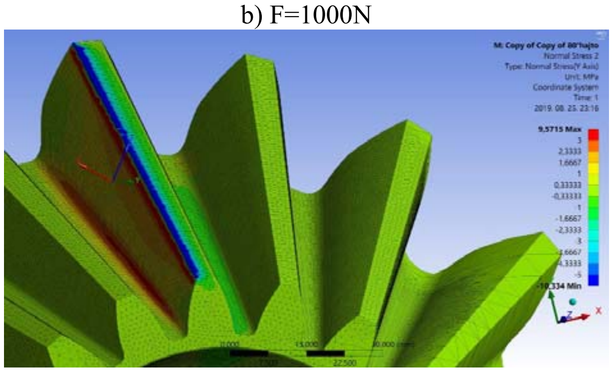

c) F=1500N

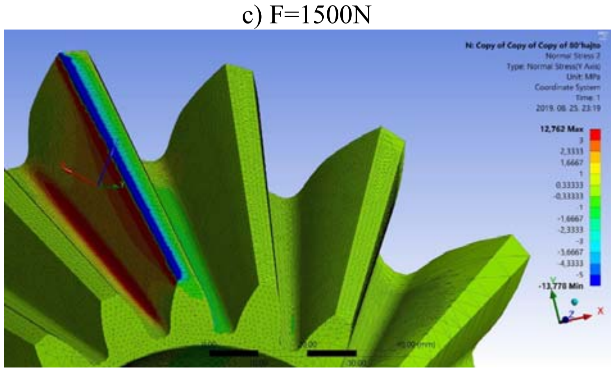

d) F=2000N

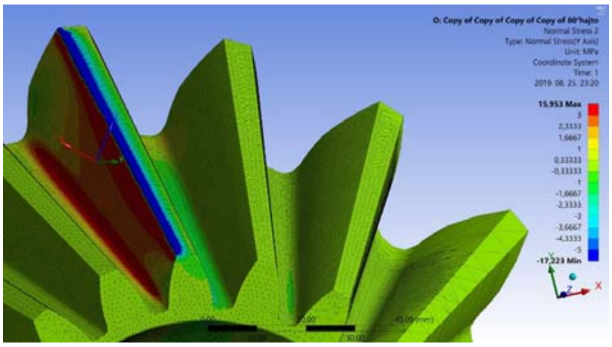

e) F=2500N

Fig. 7. The distributions of the normal stress in the function of the load forces (Σ=80°, *‘y’* direction, left side)

The results between the Σ=90° and Σ=70° arrangements can be seen on Table 4 in percentage. The deviations between the highest and lowest results are 46 % except in case of 500 N load (32 %).

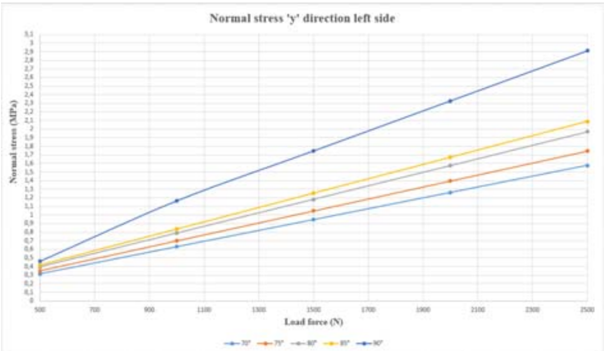

Fig. 8. The function of the normal stress and the load force for different shaft angles (*‘y’* direction, left side)

Load force (N)	Shaft angle (°)				
	70°	75°	80°	85°	90°
500	0.315	0.349	0.394	0.417	0.46
1000	0.63	0.698	0.788	0.835	1.165
1500	0.945	1.047	1.182	1.253	1.747
2000	1.261	1.396	1.576	1.671	2.329
2500	1.576	1.745	1.97	2.089	2.912

Table 3. The distributions of the *‘y’* directional normal stress (MPa) on the right side

Load force (N)	Deviation between the results (%)
500	32
1000	46
1500	46
2000	46
2500	46

Table 4. The deviations between the highest and the lowest results

2.1.3. ‘x’ direction, right side

The distributions of the normal stress into *‘x’* direction can be seen on Figure 9 on the right side. This direction is the normal direction.

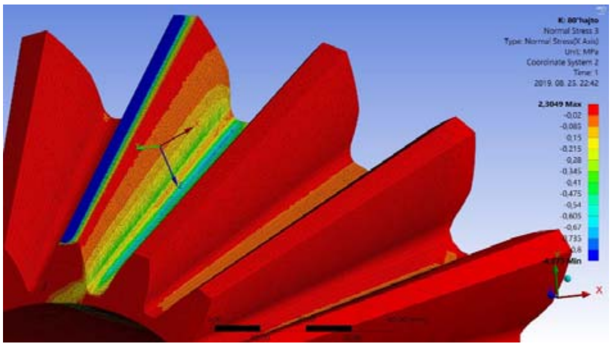

a) F=500N

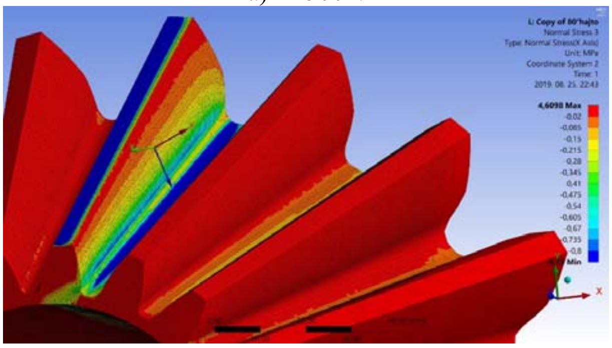

b) F=1000N

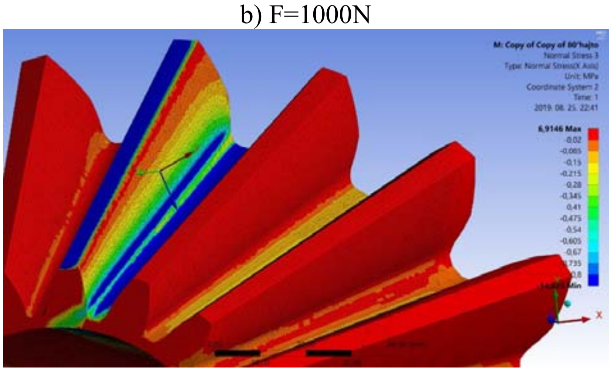

c) F=1500N

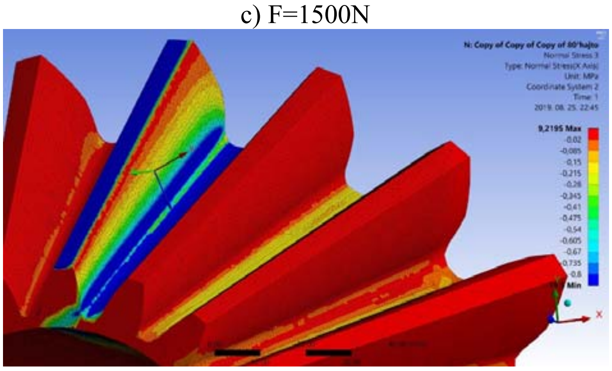

d) F=2000N

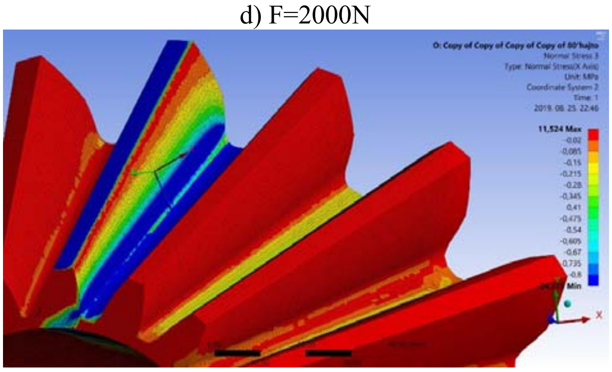

e) F=2500N

Fig. 9. The distributions of normal stress in the function of the load forces (Σ=80°, *‘x’* direction, right side)

Based on Table 5 and Figure 10 the highest normal stress values were appeared in case of Σ=75° arrangement in absolute value. The lowest normal stress values were appeared in case of Σ=90° arrangement in absolute value. The shape of the diagrams is approximately linear.

Load force (N)	Shaft angle (°)				
	70°	75°	80°	85°	90°
500	-0.0964	-0.0981	-0.0965	-0.0961	-0.0951
1000	-0.192	-0.196	-0.193	-0.192	-0.188
1500	-0.289	-0.294	-0.289	-0.288	-0.282
2000	-0.385	-0.392	-0.386	-0.384	-0.376
2500	-0.482	-0.49	-0.482	-0.48	-0.47

Table 5. The distributions of the *'x'* directional normal stress (MPa) on the left side

The results between the Σ=90° and Σ=75° arrangements can be seen on Table 6 in percentage. The deviations between the highest and lowest results are 4 % except in case of 500 N load (3 %).

Load force (N)	Deviation between the results (%)
500	3
1000	4
1500	4
2000	4
2500	4

Table 6. The deviations between the highest and the lowest results

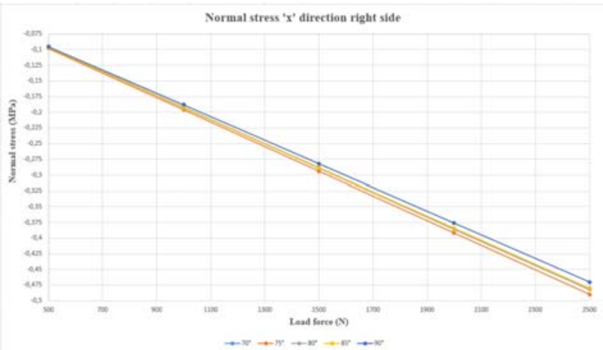

Fig. 10. The function of the normal stress and the load force for different shaft angles (*'x'* direction, right side)

2.1.4. 'y' direction, right side

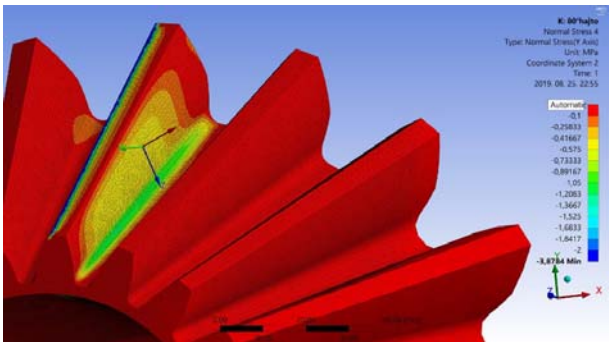

a) F=500 N

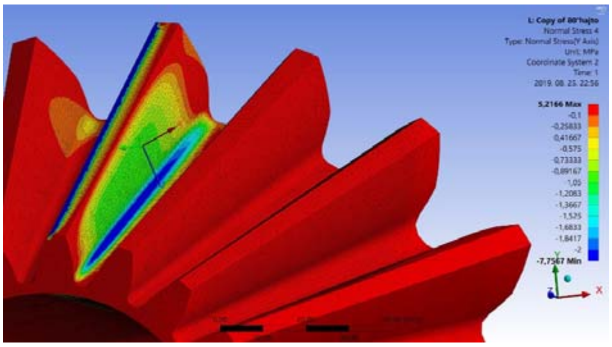

b) F=1000 N

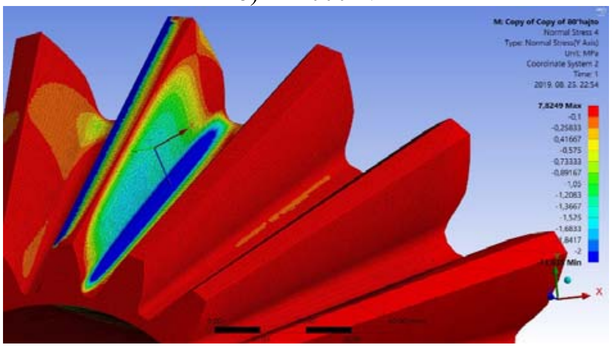

c) F=1500 N

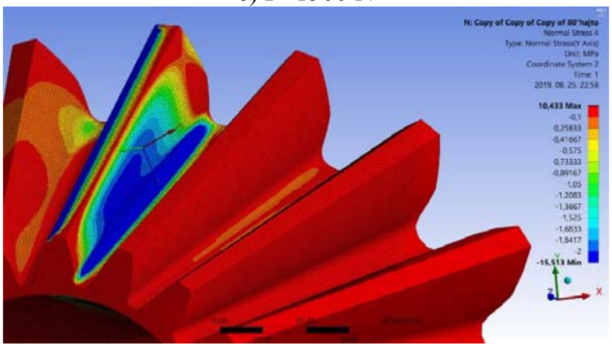

d) F=2000 N

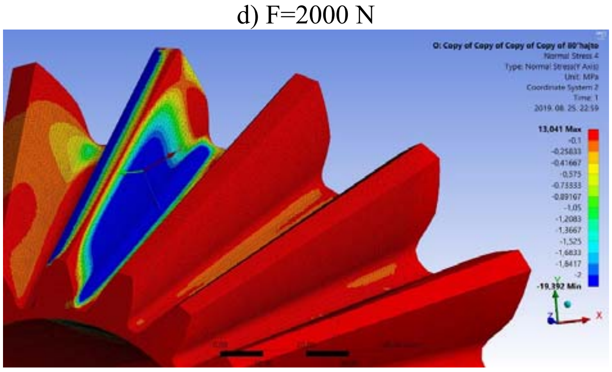

e) F=2500 N

Fig. 11. The distributions of the normal stress in the function of the load forces (Σ=80°, *'y'* direction, right side)

The distributions of normal stresses into *'y'* direction can be seen on Figure 11 on the right side. This direction is the axial direction.

Based on Table 7 and Figure 12 the highest normal stress values were appeared in case of Σ=85° arrangement in absolute value. The lowest normal stress values were appeared in case of Σ=90° arrangement except in case of 500 N load force where this case is the highest in absolute value. The shape of the diagrams is approximately linear.

The results between the Σ=90° and Σ=85°

arrangements can be seen on Table 8 in percentage. The deviations between the highest and lowest results are 22 % except in case of 500 N load (4 %).

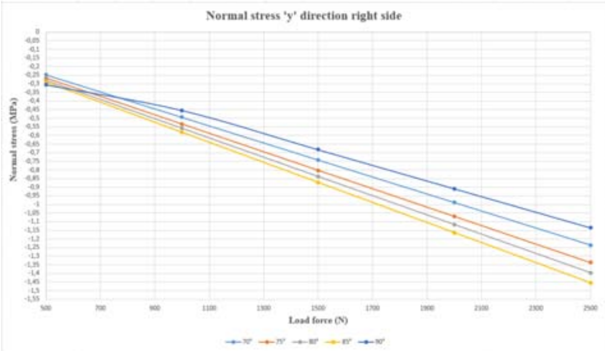

Fig. 12. The function of the normal stress and the load force for different shaft angles (*'y'* direction, right side)

Load force (N)	Shaft angle (°)				
	70°	**75°**	**80°**	**85°**	**90°**
500	-0.247	-0.267	-0.279	-0.291	-0.305
1000	-0.494	-0.534	-0.558	-0.582	-0.454
1500	-0.742	-0.802	-0.838	-0.873	-0.682
2000	-0.989	-1.069	-1.117	-1.164	-0.909
2500	-1.236	-1.337	-1.397	-1.455	-1.136

Table 7. The distributions of the *'y'* directional normal stress (MPa) on the left side

Load force (N)	Deviation between the results (%)
500	5
1000	22
1500	22
2000	22
2500	22

Table 8. The deviations between the highest and the lowest results

2.2 The analysis of the normal deformations

The normal deformations were analysed into *'x'* and *'y'* directions for both tooth sides accordingly Figure 2. Naturally this analyses were done for all of bevel gears (Σ=70°-90°).

2.2.1. 'x' direction, left side

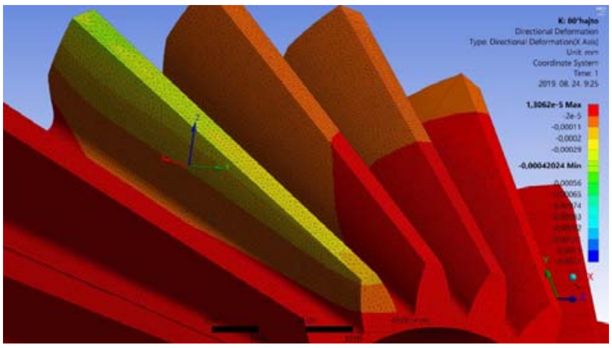

a) F=500 N

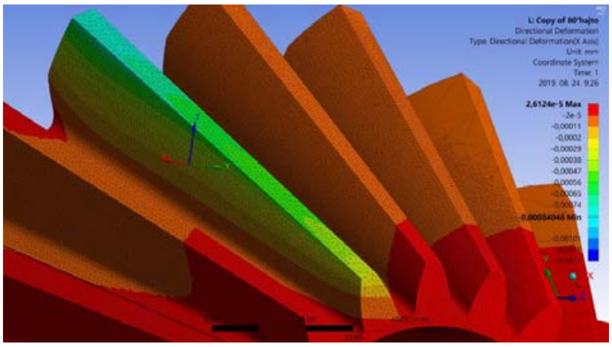

b) F=1000 N

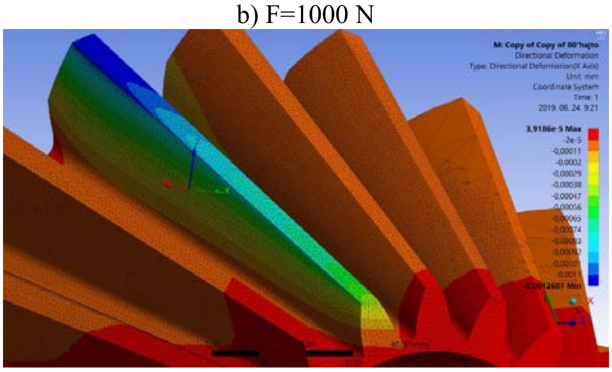

c) F=1500 N

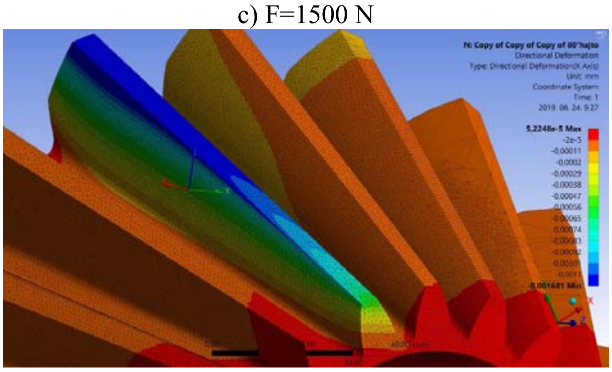

d) F=2000 N

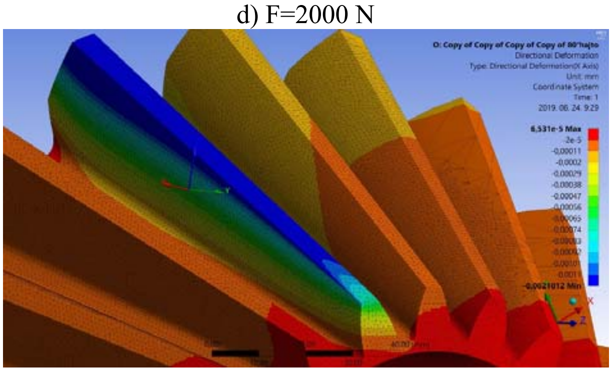

e) F=2500 N

Fig. 13. The distributions of the normal deformation in the function of the load forces (Σ=80°, *'x'* direction, left side)

Load force (N)	Shaft angle (°)				
	70°	**75°**	**80°**	**85°**	**90°**
500	-0.133	-0.132	-0.133	-0.133	-0.132
1000	-0.266	-0.265	-0.267	-0.267	-0.31
1500	-0.399	-0.398	-0.401	-0.4	-0.403
2000	-0.532	-0.531	-0.535	-0.534	-0.536
2500	-0.665	-0.664	-0.669	-0.667	-0.712

Table 9. The distributions of the *'x'* directional normal deformations (μm) on the left side

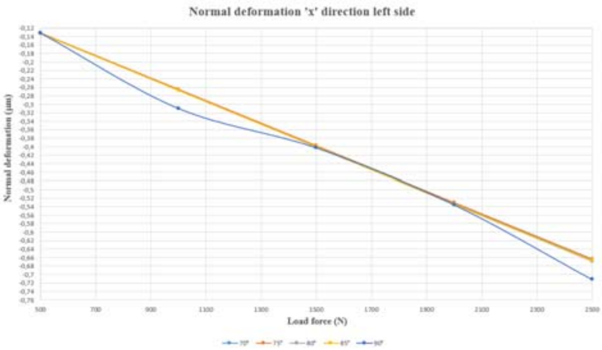

Fig. 14. The function of the normal deformation and the load force for different shaft angles (*'x'* direction, left side)

The distributions of normal stresses into 'x' direction can be seen on Figure 13 on the left side. This direction is the normal direction.

Based on Figure 14 and Table 9 the received results are mainly continuously increasing in the function of the enhancement of the shaft angle and the load force.

2.2.2. 'y' direction, left side

a) F=500 N

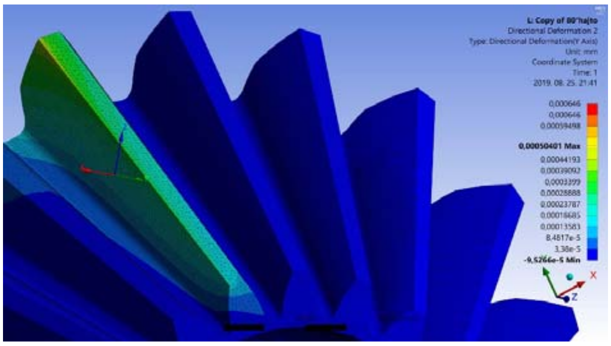

b) F=1000 N

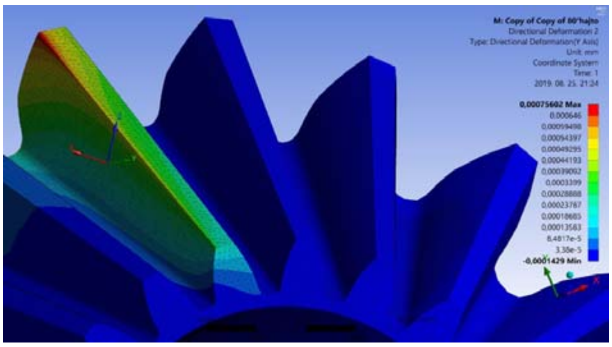

c) F=1500 N

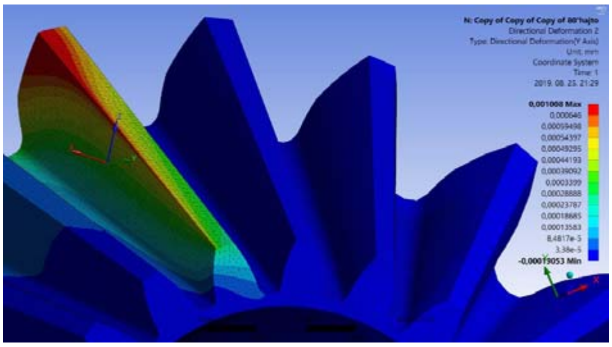

d) F=2000 N

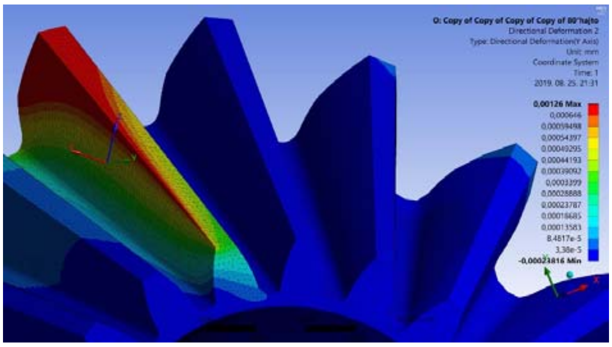

e) F=2500 N

Fig. 15. The distributions of the normal deformation in the function of the load forces (Σ=80°, 'y' direction, left side)

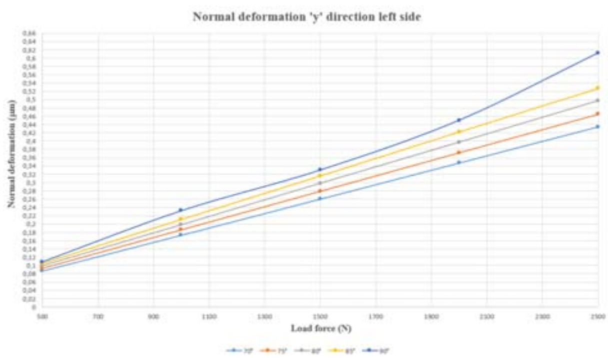

Fig. 16. The function of the normal deformation and the load force for different shaft angles (*'y'* direction, left side)

The distributions of normal deformation into *'y'* direction can be seen on Figure 15 on the left side. This direction is the axial direction.

Load force (N)	**Shaft angle (°)**				
	70°	**75°**	**80°**	**85°**	**90°**
500	0.0869	0.093	0.0994	0.105	0.109
1000	0.173	0.186	0.198	0.211	0.232
1500	0.26	0.279	0.298	0.316	0.33
2000	0.347	0.372	0.397	0.422	0.45
2500	0.434	0.465	0.497	0.527	0.612

Table 10. The distribution of the *'y'* directional normal deformation (µm) on the left side

Based on Figure 16 and Table 10 the received results are continuously increasing in the function of the enhancement of the shaft angle and the load force.

2.2.3. 'x' direction, right side

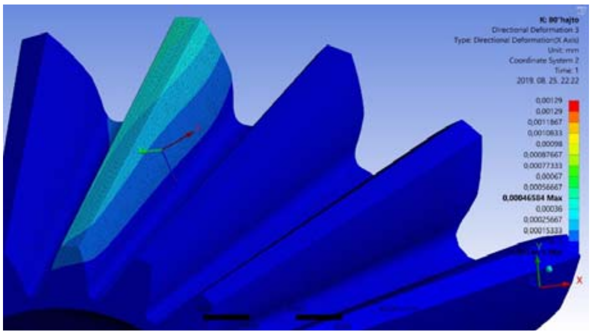

a) F=500 N

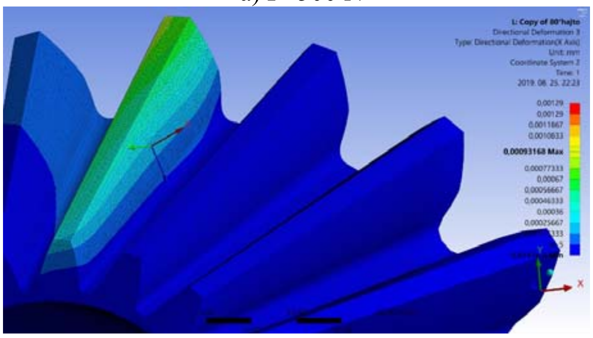

b) F=1000 N

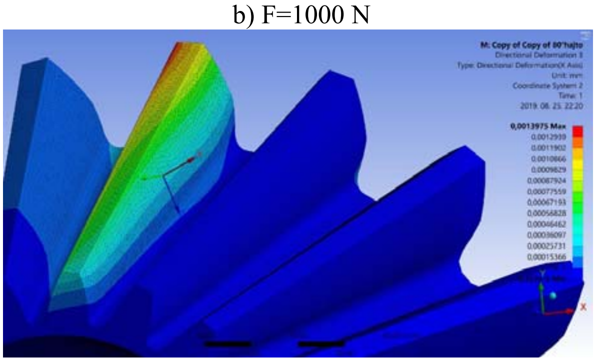

c) F=1500 N

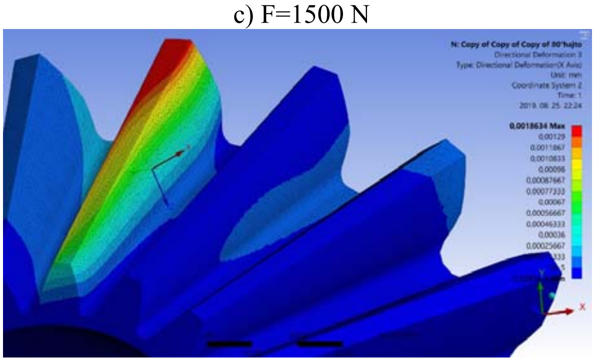

d) F=2000 N

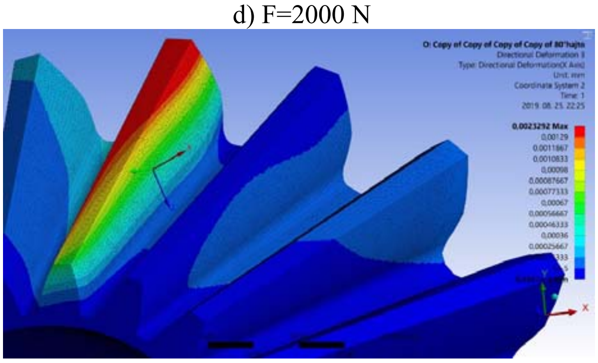

e) F=2500 N

Fig. 17. The distributions of the normal deformation in the function of the load forces (Σ=80°, *'x'* direction, right side)

The distributions of the normal deformation into *'x'* direction can be seen on Figure 17 on the right side. This direction is the normal direction.

Based on Table 11 and Figure 18 the received results are continuously increasing in the function of the enhancement of the shaft angle and the load force.

Load force (N)	**Shaft angle (°)**				
	70°	**75°**	**80°**	**85°**	**90°**
500	0.115	0.116	0.119	0.12	0.122
1000	0.231	0.233	0.238	0.24	0.242
1500	0.347	0.349	0.357	0.36	0.365
2000	0.463	0.466	0.476	0.48	0.49
2500	0.578	0.582	0.595	0.6	0.61

Table 11. The distributions of the *'x'* directional normal deformation (μm) on the right side

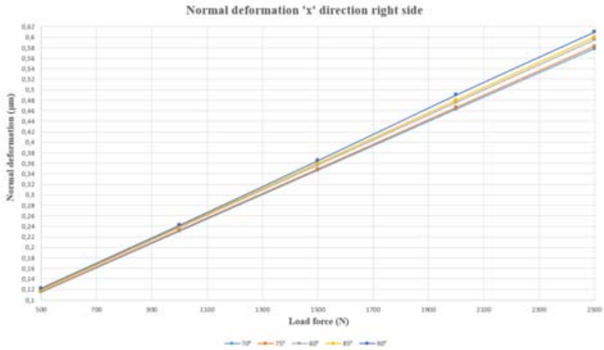

Fig 18. The function of the normal deformation and the load force for different shaft angles (*'x'* direction, right side)

2.2.4. 'y' direction, right side

The distributions of the normal deformation into 'y' direction can be seen on Figure 19 on the right side. This direction is the axial direction.

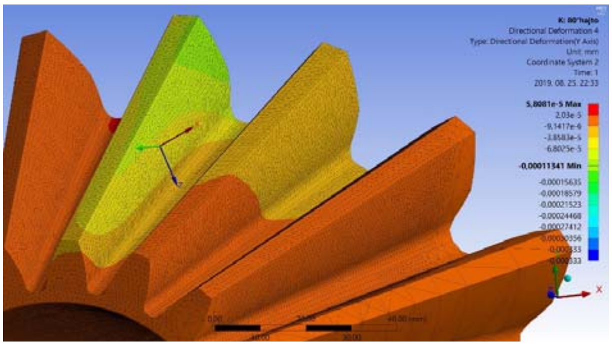

a) F=500 N

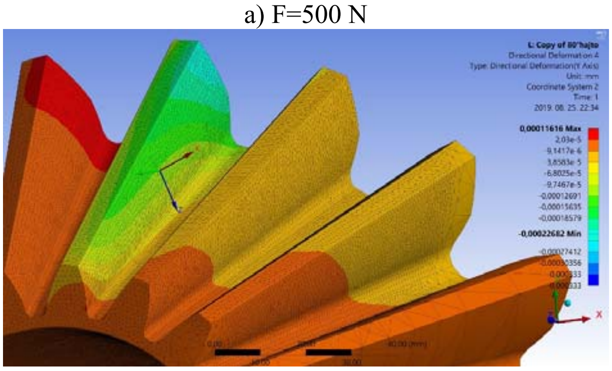

b) F=1000 N

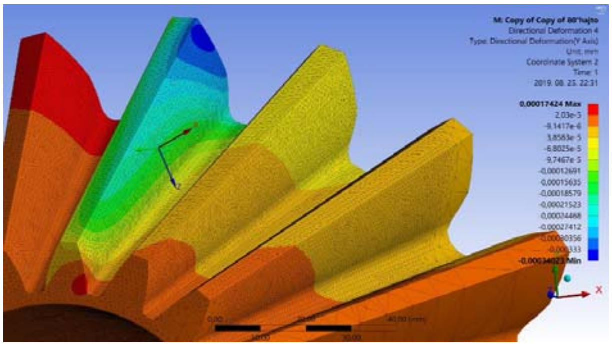

c) F=1500 N

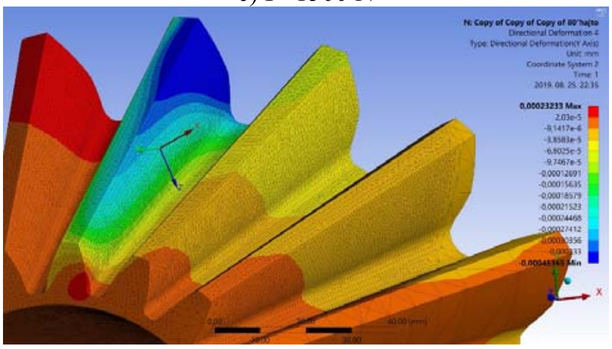

d) F=2000 N

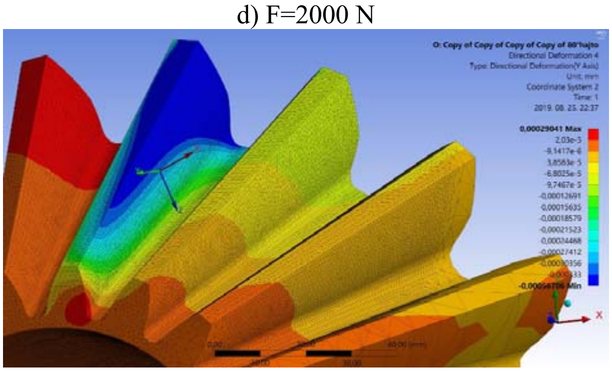

e) F=2500 N

Fig. 19. The distributions of the normal deformation in the function of the load forces (Σ=80°, *'y'* direction, right side)

Based on Table 12 and Figure 20 the received results are continuously increasing in the function of the enhancement of the shaft angle and the load force in absolute value.

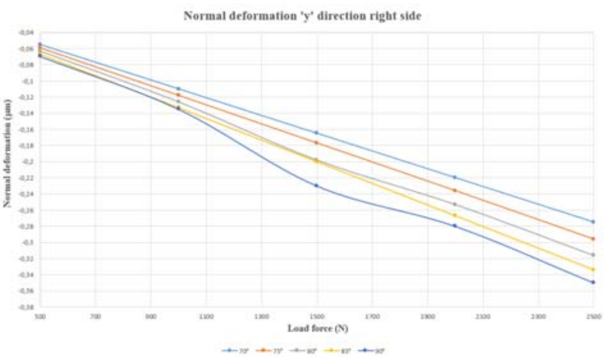

Fig. 20. The function of the normal deformation and the load force for different shaft angles (*'y'* direction, right side)

Load force (N)	Shaft angle (°)				
	70°	75°	80°	85°	90°
500	-0.0551	-0.0592	-0.0632	-0.0668	-0.0696
1000	-0.11	-0.118	-0.126	-0.133	-0.135
1500	-0.165	-0.177	-0.198	-0.2	-0.23
2000	-0.22	-0.236	-0.253	-0.267	-0.28
2500	-0.275	-0.296	-0.316	-0.334	-0.35

Table 12. The distributions of the *'y'* directional normal deformation (µm) on the right side

3. CONCLUSIONS

Five types of bevel gears having different shaft angle were designed. Geometrically these gear pairs are the same only the shaft angles are different (Σ=70°-90°). We can design them by GearTeq designer software. After that using of Solidworks software the exact connection and motion simulation can be done. In this research, we analysed the effect of the shaft angle and the load force of the pinion for the normal stresses and the normal deformations ('x' and 'y' directions on both tooth sides) by Ansys FEM software. We can find function relationship among the mechanical parameters, the load forces and the shaft angle. The necessary diagrams were created. We determined the consequences.

Naturally, our-designed bevel gear pairs can be manufactured by classical and modern (CNC) way.

ACKNOWLEDGEMENT

This research was supported by the **János Bolyai Research Scholarship of the Hungarian Academy of Sciences**.

The work/publication is partly supported by the **EFOP-3.6.1-16-2016-00022** project. The project is co-financed by the European Union and the European Social Fund.

4. REFERENCES

[1] Argyris, J., Fuentes, A., Litvin, F. L.: Computerized integrated approach for design and stress analysis of spiral bevel gears, Computer methods in applied mechanics and engineering, Elsevier, 2002, pp. 1057 - 1095

[2] Bodzás, S., Szanyi, Gy.: The Modification Effects of the Sum of Pitch Angles in Case of Bevel Gear Pairs Having Straight Teeth for the TCA, Mechanisms and Machine Science 109, Springer, pp. 97 – 109, 2022

[3] Bodzás, S.: TCA on the tooth roots of bevel gear pairs having straight teeth in the function of the modification of the shaft angles, Australian Journal of Mechanical Engineering (during publishing)

[4] Bodzás S.: Különböző típusú fogazott hajtópárok tervezése és modellezése a GearTeq szoftver alkalmazásával, Limes, A II. Rákóczi Ferenc Kárpátaljai Magyar Főiskola tudományos évkönyve (during publishing)

[5] Dudley, D. W.: „Gear Handbook", MC Graw Hill Book Co. New York-Toronto-London, 1962.

[6] Drobni, J.: Gépelemek III., Kézirat, Nemzeti Tankönyvkiadó, 1993, Miskolci Egyetem, p. 213

[7] Fangyan, Z., Mingde, Z., Weiqing, Z., Rulong, T., Xiaodong, G.: On the deformed tooth contact analysis for forged bevel gear modification, Mechanism and Machine Theory, Elsevier, 2019, Volume 135, pp. 192-207, https://doi.org/10.1016/j.mechmachtheory.2019.01.024

[8] Fuentes A., A., Iserte J. L., Gonzalez P., I., Sanchez M., F. T.: Computerized design of advanced straight and skew bevel gears produced by precision forging, Computer methods in applied mechanics and engineering, Elsevier, 2011, pp. 2363 - 2377

[9] Fuentes A., A., Yague M., E., Gonzalez P., I.: Computerized generation and gear mesh simulation of straight bevel gears manufactured by dual interlocking circular cutters, Mechanism and Machine Theory, Elsevier, 2018, pp. 160-176

[10] Goldfarb, V., Trubachev, E., Barmina, N.: Advanced Gear Engineering, Springer, 2018, p. 197., ISBN 978-3-319-60398-8

[11] Gołębski, R., Szarek, A.: Diagnosis of the Operational Gear Wheel Wear Technical Gazette, 26(3), 658-661., 2019, https://doi.org/10.17559/TV-20180321171428

[12] Litvin, F. L., Fuentes A., A.: Gear Geometry and Applied Theory, Cambridge University Press, 2004., ISBN 978 0 521 81517 8

[13] Moaveni S.: Finite Element Analysis, Theory and Application with ANSYS, Pearson Education Limited, 2015, ISBN 10: 0-273-77430-1, p. 928

[14] Peng, S., Ding, H., Zhang, G., Tang, J., Tang, Y.: New determination to loaded transmission error of the spiral bevel gear considering multiple elastic deformation evaluations under different bearing supports, Mechanism and Machine Theory, Elsevier, 2019, Volume 137, pp. 37-52, https://doi.org/10.1016/j.mechmachtheory.2019.03.013

[15] Radzevich, Stephen P.: Dudley's Handbook of Practical Gear Design and Manufacture, Third Edition, CRC Press, Taylor & Francis Group, 2016, ISBN 978-1-4987-5310-4, p. 615

[16] Samani, F. S., Molaie, M., Pellicano F.: Nonlinear vibration of the spiral bevel gear with a novel tooth surface modification method, Meccanica, Springer, 2019, Volume 54, Issue 7, pp. 1071-1081

[17] Zehua, H., Han, D., Shandong, P., Yi, T., Jinyuan, T.: Numerical determination to loaded tooth contact performances in consideration of misalignment for the spiral bevel gears, Mechanism and Machine Theory, Elsevier, 2019, Volume 151, pp. 343-355, https://doi.org/10.1016/j.ijmecsci.2018.11.014

[18] Zeng, Q. L., Wang, K., Wan, L. R.: Modelling and straight bevel gear transmission and simulation of its meshing performance, Int j simul model 17, 2018, ISSN 1726-4529

[19] Zolfaghari A., Goharimanesh M., Akbar Akbari A.: Optimum design of straight bevel gears pair using evolutionary algorithms, The Brazilian Society of Mechanical Sciences and Engineering, Springer, 2017, pp. 2121-2129, DOI 10.1007/s40430-017-0733-9

[20] Wagner, W., Schumann, S., Schlecht, B.: Co-simulation of the tooth contact of bevel gears within a multibody simulation, Springer, 2019, Volume 83, Issue 3, pp. 425-433

[21] Terplán, Z.: Gépelemek IV., Kézirat, Tankönyvkiadó, Budapest, 1975, p. 220.

Author: **Dr. Sándor Bodzás, Ph.D.,** Deputy head of department, Associate professor, Department of Mechanical Engineering, University of Debrecen**,** Debrecen, Ótemető str. 2-4, 4028, Hungary.
E-mail: bodzassandor@eng.unideb.hu